Heatsink-free CW operation of injection microdisk lasers grown on Si substrate with emission wavelength beyond 1.3 μm

NATALIA KRYZHANOVSKAYA,[1,3,*] EDUARD MOISEEV,[1] YULIA POLUBAVKINA,[1] MIKHAIL MAXIMOV,[1,2] MARINA KULAGINA,[2] SERGEY TROSHKOV,[2] YURY ZADIRANOV,[2] YULIA GUSEVA,[2] ANDREY LIPOVSKII,[1,3] MINGCHU TANG,[4] MENGYA LIAO,[4] JIANG WU,[4] SIMING CHEN,[4] HUIYUN LIU,[4] ALEXEY ZHUKOV[1,3]

[1] *Nanophotonics Lab, St Petersburg Academic University, 194021 St Petersburg, Russia*
[2] *Ioffe Physical Technical Institute of RAS, 194021 St Petersburg, Russia*
[3] *Peter the Great St Petersburg Polytechnic University, 195251 St Petersburg, Russia*
[4] *Department of Electronic and Electrical Engineering, University College London, London WC1E 7JE, UK*
**Corresponding author: NataliaKryzh@gmail.com*

Received XX Month XXXX; revised XX Month, XXXX; accepted XX Month XXXX; posted XX Month XXXX (Doc. ID XXXXX); published XX Month XXXX

High-performance injection microdisk lasers grown on Si substrate are demonstrated for the first time. Continuous wave lasing in microlasers with diameters from 14 to 30 μm is achieved at room temperature. The minimal threshold current density of 600 A/cm² (room temperature, continuous wave regime, heatsink-free uncooled operation) is comparable to that of high-quality microdisk lasers on GaAs substrates. Microlasers on silicon emit in the wavelength range of 1320-1350 nm via the ground state transition of InAs/InGaAs/GaAs quantum dots. High stability of the lasing wavelength (dλ/dI=0.1 nm/mA) and low specific thermal resistance of 4×10^{-3} °C×cm²/W are demonstrated.

OCIS codes: *(140.5960 Semiconductor lasers; 230.5590 Quantum-well, -wire and -dot devices; (140.3945 Microcavities).*

http://dx.doi.org/10.1364/OL.99.099999

Realization of compact silicon-based lasers capable for reliable operation at elevated temperatures is a subject of persistent attempts of many research groups worldwide. To date, several approaches have been proposed to realize light source on silicon. This includes the hybrid III-V-silicon integration, that can be done using different bonding techniques such as flip-chip bonding [1] or molecular bonding [2,3]. For this purpose, InP-based laser structures with InAsP/InGaAsP quantum wells (QWs) were used. The highest operation temperature for InP-based microring lasers with a diameter of 50 μm is 65°C[4]. For further increase of the operating temperature (up to 105C) a special thermal shunt design improving thermal conductivity is required [5]. The highest operating temperature of InP-based microlasers is limited by small energy of the carrier confinement in the active region (small conduction band offsets). Moreover, it is often in bonded structures that the major part of the optical field is located in the silicon waveguide and its overlap with the III-V active region is only a few percents. Another group of integration methods is based on direct epitaxial growth of III-V active layers on silicon substrates. An approach based on Ge/Si (001) virtual substrate [6] has been recently used to achieve room-temperature lasing in InGaAs/GaAs quantum well microdisk (MD) lasers with 23 μm diameter [7]. The minimal threshold current density was 28 kA/cm² reflecting a high sensitivity of a quantum well active region to various defects originated from both epitaxial growth on silicon and damaged microresonator sidewalls. In this respect quantum dots (QDs) can offer advantageous characteristics owing to a suppressed lateral transport of charge carriers which prevents their diffusion towards non-radiate recombination centers. Owing to this unique property of QDs, a significant progress has been demonstrated in the past years in realization of III-V-Si injection lasers [8–10]. A low density of threading dislocations on the order of 10^5 cm^{-2} in the III–V epilayers grown on silicon (100)-oriented substrates with 4° offcut is achieved by combining a nucleation layer and dislocation filter layers with in situ thermal annealing. Continuous-wave (CW) InAs/GaAs QD lasers directly grown on silicon substrates with a low threshold current density (J_{th}) of 62.5 A/cm² at room-temperature and operation up to 120 °C has been demonstrated [10]. Nevertheless, there were only few publications on realization of optically-pumped III-V microlasers monolithically

grown on silicon [11–13]. Very recently the first electrically pumped microring lasers with InAs/InGaAs quantum dots active region grown on a V-groove patterned (001) silicon have been demonstrated [14]. A multimode operation with central wavelength near 1.3 μm was achieved in CW regime for microring lasers as small as 10 μm in diameter; the maximum operation temperature up to 100°C was demonstrated for a microring laser with diameter of 100 μm. This correlates well with 100°C operation of QD MD lasers grown on GaAs substrate [15].

Prospective applications of light emitters on silicon require high stability of emission wavelength. Locking a lasing wavelength to a whispering gallery mode resonance, as it usually occurs in MD/microring optical cavities, leads to a reduced sensitivity of lasing wavelength to temperature variation as compared to macrolasers [16]. However, current-induced wavelength shift caused by a device self-heating can be a significant problem for uncooled microlasers operating in CW regime. Owing to better heat dissipation, microdisk lasers can provide better performance in comparison with their microring counterparts. Compared to microrings, resonators with MD geometry can readily be scaled further down to extremely small diameters of 1 μm [17]. In this Letter, we report on CW lasing of uncooled electrically-pumped microdisk lasers monolithically grown on Si substrates. Under DC injection, lasing is achieved at room temperature in microlasers with diameters of 14, 18 and 30 μm with a minimal threshold current density of 600 A/cm^2. The InAs/InGaAs dot-in-well (DWELL) active region provides the wavelengths in the 1.32–1.35 μm spectral interval. Single mode emission is demonstrated with a dominant mode linewidth as narrow as 30 pm.

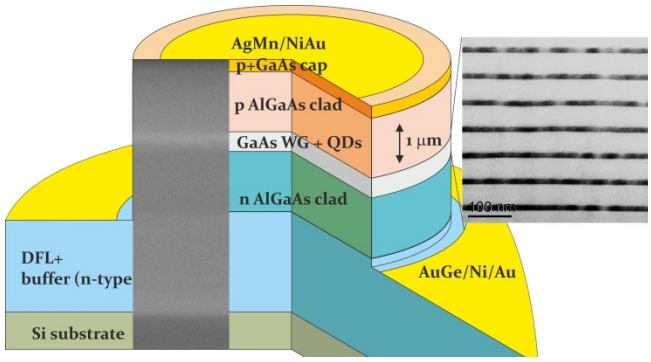

Fig. 1. Schematic of the layer sequence. The left inset shows a scanning electron microscopy image of the structure cross-section; the right inset shows a bright-field transmission electron microscopy image of the QD active layers.

A III-V QD laser structure was directly grown on a n-doped silicon (001) substrate with 4° offcut to the [011] plane by solid-source molecular beam epitaxy (MBE). Oxide desorption was first performed by holding the silicon substrate at a temperature of 900°C for 10 min. Epitaxy was then carried out in the following order illustrated in Fig. 1: a 30nm AlAs nucleation layer, a 570nm GaAs buffer layer, a 50-period $Al_{0.4}Ga_{0.6}As$/GaAs superlattice of 200 nm, a 100 nm GaAs buffer layer, InGaAs/GaAs dislocation filter layers (DFL) [18], a 25-period bottom $Al_{0.4}Ga_{0.6}As$/GaAs superlattice of 50 nm, 7 layers of InAs/InGaAs DWELL structures separated by 38.5 nm GaAs spacers in the middle of a 140 nm undoped GaAs waveguide layer embedded between 1.4μm n-type lower and p-type upper $Al_{0.4}Ga_{0.6}As$ cladding layers, a 25-period upper $Al_{0.4}Ga_{0.6}As$ /GaAs superlattice of 50 nm, and finally, a 300nm highly p-doped GaAs contacting layer. Good planarity of interfaces and a nearly defect-free DWELL active region is achieved (Insets of Fig. 1). The typical dot size is ~20 nm in diameter and ~7 nm in height. A good QD uniformity is obtained with a density of ~3 × 10^{10} cm^{-2} for an uncapped QD sample grown on Si under exactly the same conditions (Inset of Fig. 2).

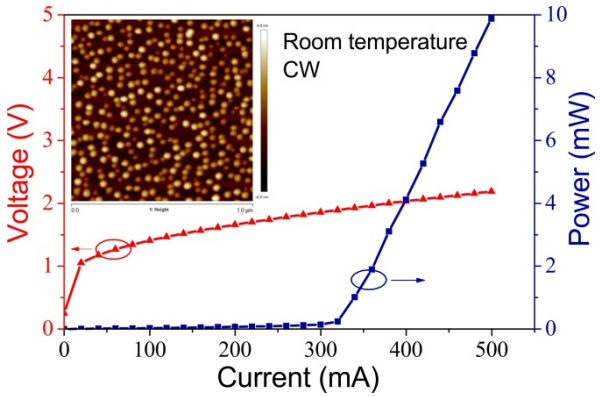

Fig. 2. L-I-V characteristics for a 25μm × 3 mm edge-emitting QD laser grown on Si under cw operation at room temperature. Inset: Representative atomic force microscopy image of uncapped QD sample grown on silicon.

To evaluate the performance of QD material directly grown on silicon substrate, the heterostructure was processed into broad-area lasers with as-cleaved facets and ridges of 25 μm in width and 3 mm in length. No facet coating was applied. The lasers were mounted p-side up and wire bonded on a copper block to enable testing. Fig. 2 shows the typical light-current-voltage (L-I-V) characteristics for the QD laser grown directly on silicon under CW operation at room temperature. A threshold current (I_{th}) of 320 mA (J_{th} = 427 A/cm^2) is observed. The measured single facet output power is 10 mW at an injection current of 500 mA, with no evidence of power saturation up to this current. A series resistance is 2 Ohm with a turn-on voltage of 1.22 V. The light emission spectrum measured slightly above the threshold current (350 mA) reveals the lasing wavelength of 1318 nm. For the edge-emitting QD-on-Si laser of similar layered design and growth procedure, a mean time to failure of over 100 000 hours has been determined [10].

For MD lasers, circular mesas with diameters of 14, 18, and 30 μm were defined by photolithography and dry etching. The mesa height was chosen about 4.5 μm to ensure optical confinement of the resonator modes. No sidewall coating or passivation was applied. AgMn/NiAu (AuGe/Ni/Au) metallization was used for formation of ohmic contacts to the p+ GaAs cap layer (the underlying n-doped GaAs layer, respectively). A micrograph of a 30-μm microlaser is shown in the inset of Fig. 3. All the microlasers demonstrated distinct turn-on behavior of I-V characteristic. The estimated series resistance increases from ~100 to ~250 Ohm as the device diameter decreases from 30 to 14 μm. MD lasers were mounted on a sample holder to be tested at room temperature in CW regime with a DC current varied from 0 to 50 mA. Needle probes were used for electrical connections. No heatsink soldering or fan cooling was employed. A piezoelectrically adjustable

Olympus LMPlan IR objective x10 was used to collect in-plane emitted light from a microlaser. The emission was detected with a Horiba FHR 1000 monochromator and a Horiba Symphony InGaAs CCD matrix. The spectral resolution was 30 pm.

All the microlasers demonstrate emission spectra with the peak wavelengths falling into the spectral interval well beyond 1.3 μm. Fig. 3 depicts representative lasing spectra from MD lasers with diameters of 14 and 30 μm, respectively. In the 14-μm device, a dominant line is located at 1351 nm. To the best of our knowledge, this is the longest lasing wavelength ever reported for injection QD microlasers on silicon substrate. The neighboring less intense cavity mode is blue-shifted by 10.7 nm from the dominant mode. Taking into account this free spectral range (FSR) together with the FSR data obtained for larger diameters, an effective mode index of 3.8 was estimated. The spectra shown in Fig.3 (as well as for the other tested microlasers) are nearly singlemode in a wide range of injection currents with the peak-to-peak side mode suppression ratio of 20 dB and above. The lasing wavelengths are red shifted with respect to the room temperature photoluminescence peak of QD material, which is located at 1297 nm (dotted line in Fig. 3). No lasing line can be found in spectral interval of excited state optical transition around 1.2 μm.

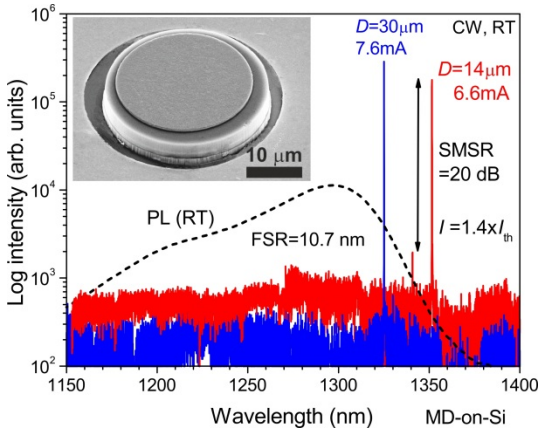

Fig. 3. Room-temperature CW emission spectra taken at current of ~1.4 x threshold for MD-on-Si lasers with diameters of 14 and 30 μm. Dashed curve: photoluminescence spectrum of QD material (not in scale). Inset: SEM image of the MD laser (D = 30 μm).

The laser operation is confirmed by a pronounced knee in the L-I curve and by sudden linewidth narrowing. Upon reaching the lasing threshold, full width at half maximum (FWHM) of the dominant line drops down to 30±4 pm, which is the resolution limit of our spectral system. An example is presented in Fig. 4(a) for the 1321 nm mode of a microlaser with a diameter of 30 μm. This cavity line remains the dominant one up to injection current of 30 mA. Further growth of current leads to a jump of lasing mode to another cavity resonance at 1370 nm.

The integrated line intensity of the 1321 nm mode is shown as a function of injection current in Fig. 4(a) in a double logarithmic scale. The I_{th} is estimated at 4.2 mA, corresponding to a J_{th} of 594 A/cm^2, which is only 1.4 times higher than the value of J_{th} measured in the broad-area laser. This is a direct evidence of suppression of nonradiative recombination at deeply etched sidewalls of the quantum dot structure [19]. In contrast to QDs, two-dimensional quantum wells usually require passivation to enable room temperature operation [20]. For example, in an InGaAs quantum well MD laser on silicon, the threshold current density rises by a factor of 5 as compared to a macrolaser made of the same epitaxial structure [7]. It is also worth mentioning that the threshold current density achieved in the present work for MD lasers on silicon is half the value of J_{th} (1.2 kA/cm^2) published for a micro-ring laser on silicon substrate with a radius of 50 μm [17].

Fig. 4(b) summarizes the threshold current data obtained in the present work for MD lasers of different diameters. The smallest I_{th} of 2.4 mA was measured for a MD laser with the diameter of 18 μm. This is in a good agreement with the threshold currents measured in QD based MD lasers on GaAs substrate with comparable disk diameters [21]. Those data are also presented in Fig. 4(b). Although a gradual decrease of I_{th} with decreasing the device area is expected if the threshold current density remains unchanged, we however observed a non-monotonic dependence of the threshold current on diameter in our uncooled MD lasers. As is seen in Fig. 4(b), the smallest microdisks (14 μm in diameter) are characterized by higher I_{th} of 4.7 mA. This can be associated, at least partly, with microlasers self-heating.

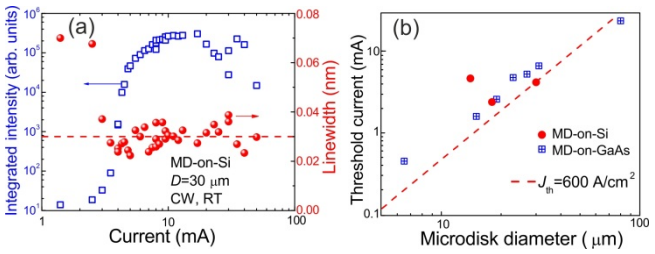

Fig. 4. (a) Current dependence of integrated line intensity (squares) and FWHM (circles) for the 1321.5 nm mode of a 30 μm MD laser. Dashed line represents the spectral resolution; (b) Circles: Minimal threshold current of MD-on-silicon as a function of diameter. Dashed line: threshold current expected for a constant J_{th} of 600 A/cm^2. Squares: data on I_{th} versus diameter for QD-based MD lasers on GaAs extracted from Refs [21–23].

Fig. 5(a) illustrates spectral position of the lasing modes against injection current for the MD-on-Si microlasers of two different diameters, 14 and 30 μm. The current-induced mode redshift is caused by self-heating of uncooled devices operating in CW regime. The slope coefficient (dλ/dI) of 0.5 and 0.1 nm/mA was estimated for the microlasers of smaller and larger diameters, respectively. The temperature variation of a mode position is described by the coefficient (dλ/dT) = 81.5 pm/°C as it was evaluated for QD-on-GaAs MD of similar geometry and spectral band [15]. Therefore, the smaller microlaser is additionally heated by about 30°C at its threshold current. For the larger one, microlaser self-heating at the threshold is only ~5°C. In the former case, a reduced area of the MD footprint leads to higher thermal resistance (TR) as compared to the latter one. This effect is presumably responsible for a noticeably longer lasing wavelength in the MD laser with the diameter of 14 μm.

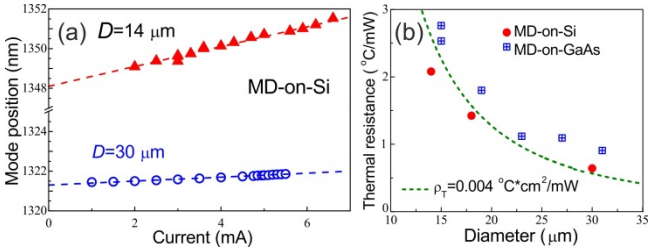

Fig. 5. (a) Lasing wavelength vs current for the MD-on-Si with diameters of 14 and 30 μm (triangles and circles, respectively). Dashed lines: Linear fit; (b) Circles: Average thermal resistance of MD-on-silicon lasers as a function of diameter. Dashed curve: TR expected for a constant specific thermal resistance of 4×10^{-3} $^{o}C\times cm^2/mW$. Squares: data on TR versus diameter for QD-based MD lasers on GaAs extracted from Ref. [21].

Combining ($d\lambda/dI$) and ($d\lambda/dT$) coefficients with I-V characteristics, we evaluated TR of the MD-on-Si lasers under study. Results are presented in Fig. 5(b). As the MD diameter decreases in the given interval, TR increases from ~0.64 to ~2.1 $^{o}C/mW$. This approximately corresponds to a specific thermal resistance (normalized to the device footprint area) of 4×10^{-3} $^{o}C\times cm^2/mW$. The TR data obtained for MD-on-GaAs of similar design are shown in Fig. 5(b) for the sake of comparison. It is seen that MD lasers with (Al)GaAs cavity are characterized by very close values of thermal resistance regardless of a substrate used (either Si or GaAs). It should be noted that specific thermal resistance of InGaAsP–InP MD lasers are several times higher ([24] and references herein).

In conclusion, MD lasers with small footprint were made of a laser heterostructure monolithically grown on silicon substrate. No modification of the layer/composition design is required compared to conventional edge-emitting lasers. Simple post-growth process with a single-step lithography and a standard dry etching procedure were applied. No sidewall passivation or other protection was used. These microlasers are capable of operating in CW regime without external cooling or soldering to a heatsink. Emission spectra are characterized by a narrow dominant line, of which the peak intensity exceeds intensities of neighboring modes/background by at least two orders of magnitude. The line width in lasing regime is as narrow as 30 pm, which is in fact a spectral resolution limit. The lasing peak is spectrally positioned well beyond 1.3 μm (1.32–1.35 μm) and demonstrates low sensitivity to current-induced self-heating. The threshold and thermal properties of the microlasers on silicon are comparable to or even better than the characteristics obtained on high-quality QD microlasers on GaAs substrate. The obtained set of device characteristics makes them promising as a building block for future nanophotonic emitters integrated on silicon chips.

Funding. This work was supported by the Russian Foundation for Basic Research (16-29-03037, 16-29-03111), Russian Ministry of Education and Science (3.9787.2017/8.9) and by UK EPSRC (EP/J012904/1), (EP/K029118/1), (EP/P006973/1).

References

1. K. Kato and Y. Tohmori, IEEE J. Sel. Top. Quantum Electron. **6**, 4 (2000).
2. J. Van Campenhout, L. Liu, P. Rojo Romeo, D. Van Thourhout, C. Seassal, P. Regreny, L. Di Cioccio, J. Fedeli, and R. A. Baets, IEEE Photon. Tech. Lett. **20**, 1345 (2008).
3. B. Ben Bakir, A. Descos, N. Olivier, D. Bordel, P. Grosse, E. Augendre, L. Fulbert, and J.-M. Fedeli, Opt. Express **19**, 10317 (2011).
4. D. Liang, M. Fiorentino, S. Srinivasan, J. E. Bowers, and R. G. Beausoleil, IEEE J. Sel. Top. Quantum Electron. **17**, 1528 (2011).
5. C. Zhang, D. Liang, G. Kurczveil, J. E. Bowers, and R. G. Beausoleil, IEEE J. Sel. Top. Quantum Electron. **21**, 1502607 (2015).
6. V. Ya. Aleshkin, N. V. Baidus, A. A. Dubinov, A. G. Fefelov, Z. F. Krasilnik, K. E. Kudryavtsev, S. M. Nekorkin, A. V. Novikov, D. A. Pavlov, I. V. Samartsev, E. V. Skorokhodov, M. V. Shaleev, A. A. Sushkov, A. N. Yablonskiy, P. A. Yunin, and D. V. Yurasov, Appl. Phys. Lett. **109**, 061111 (2016).
7. N. V. Kryzhanovskaya, E. I. Moiseev, Yu. S. Polubavkina, M. V. Maximov, M. M. Kulagina, S. I. Troshkov, Yu. M. Zadiranov, A. A. Lipovskii, N. V. Baidus, A. A. Dubinov, Z. F. Krasilnik, A. V. Novikov, D. A. Pavlov, A. V. Rykov, A. A. Sushkov, D. V. Yurasov, and A. E. Zhukov, Opt. Express **25**, 16754 (2017).
8. T. Wang, H. Liu, A. Lee, and F. Pozzi, A. Seeds, Opt. Express **19**, 11381 (2011).
9. A. D. Lee, Q. Jiang, M. Tang, Y. Zhang, A. J. Seeds, and H. Liu, IEEE J. Select. Topics Quantum Electron. **19**, 1901107 (2013).
10. S. Chen, W. Li, J. Wu, Q. Jiang, M. Tang, S. Shutts, S. N. Elliott, A. Sobiesierski, A. J. Seeds, I. Ross, P. M. Smowton, and H. Liu, Nat. Photon. **10**, 307 (2016).
11. R. Chen, T. T. D. Tran, K. W. Ng, W. S. Ko, L. C. Chuang, F. G. Sedwick, and C. J. Chang-Hasnain, Nat. Photon. **5**, 170 (2011).
12. T. T. D. Tran, R. Chen, K. W. Ng, W. S. Ko, F. Lu, and C. J. Chang-Hasnain, Appl. Phys. Lett. **105**, 111105 (2014).
13. Y. Wan, Q. Li, A. Y. Liu, and A. C. Gossard, J. E. Bowers, E. Hu, and K. M. Lau, Opt. Lett. **41**, 1664 (2016).
14. Y. Wan, J. Norman, Q. Li, M. J. Kennedy, D. Liang, C. Zhang, D. Huang, A. Y. Liu, A. Torres, D. Jung, A. C. Gossard, E. L. Hu, K. M. Lau, and J. E. Bowers, CLEO: Applications and Technology 2017, San Jose, CA, USA, May 14–19, 2017, paper JTh5C.3.
15. N. V. Kryzhanovskaya, E. I. Moiseev, Yu. V. Kudashova, F. I. Zubov, A. A. Lipovskii, M. M. Kulagina, S. I. Troshkov, Yu. M. Zadiranov, D. A. Livshits, M. V. Maximov, and A. E. Zhukov, Electron. Lett. **51**, 1354 (2015).
16. M. V. Maximov, N. V. Kryzhanovskay, A. M. Nadtochiy, E. I. Moiseev, I. I. Shostak, A. A. Bogdanov, Z. F. Sadrieva, A. E. Zhukov, A. A. Lipovskii, D. V. Karpov, J. Laukkanen, and J. Tommila, Nanoscale Res. Lett. **9**, 657 (2014).
17. N. V. Kryzhanovskaya, A. E. Zhukov, M. V. Maximov, E. I. Moiseev, I. I. Shostak, A. M. Nadtochiy, Yu. V. Kudashova, A. A. Lipovskii, M. M. Kulagina, and S. I. Troshkov, IEEE J. Select. Topics Quantum Electron. **21**, 1900905 (2015).
18. M. Tang, S. Chen, J. Wu, Q. Jiang, K. Kennedy, P. Jurczak, M. Liao, R. Beanland, A. J. Seeds, and H. Liu, IEEE J. Sel. Top. Quantum Electron. 22, 1900207 (2016).
19. D. Ouyang, N. N. Ledentsov, D. Bimberg, A. R. Kovsh, A. E. Zhukov, S. S. Mikhrin, and V. M. Ustinov, Semicond. Sci. Technol. **18**, L53 (2003).
20. N. V. Kryzhanovskaya, E. I. Moiseev, Yu. S. Polubavkina, F. I. Zubov, M. V. Maximov, A. A. Lipovskii, M. M. Kulagina, S. I. Troshkov, V.-M. Korpijarvi, T. Niemi, R. Isoaho, M. Guina, M. V. Lebedev, T. V. Lvova, and A. E. Zhukov, J. Appl. Phys. **120**, 233103 (2016).
21. N. V. Kryzhanovskaya, M. V. Maximov, S. A. Blokhin, M. A. Bobrov, M. M. Kulagina, S. I. Troshkov, Yu. M. Zadiranov, A. A. Lipovskii, E. I. Moiseev, Yu. V. Kudashova, D. A. Livshits, V. M. Ustinov, and A. E. Zhukov, Semiconductors **50**, 390 (2016).
22. M.-H. Mao, H.-C. Chien, J.-Z. Hong, and C.-Y. Cheng, Opt. Express **19**, 14145 (2011).
23. M. Munsch, J. Claudon, N. S. Malik, K. Gilbert, P. Grosse, J.-M. Gerard, F. Albert, F. Langer, T. Schlereth, M. M. Pieczarka, S. Hofling, M. Kamp, A. Forchel, and S. Reitzenstein, Appl. Phys. Lett. **100**, 031111 (2012).
24. A. E. Zhukov, N. V. Kryzhanovskaya, M. V. Maximov, A. A. Lipovskii, A. V. Savelyev, I. I. Shostak, E. I. Moiseev, Yu. V. Kudashova, M. M. Kulagina, and S. I. Troshkov, Semiconductors **49**, 674 (2015).

References

1. K. Kato and Y. Tohmori, PLC hybrid integration technology and its application to photonic components. IEEE J. Select. Topics Quantum Electron. **6**, 4 (2000).
2. J. Van Campenhout, L. Liu, P. Rojo Romeo, D. Van Thourhout, C. Seassal, P. Regreny, L. Di Cioccio, J. Fedeli, and R. A. Baets, A compact SOI-integrated multiwavelength laser source based on cascaded InP microdisks. IEEE Photon. Tech. Lett. **20**, 1345 (2008).
3. B. Ben Bakir, A. Descos, N. Olivier, D. Bordel, P. Grosse, E. Augendre, L. Fulbert, and J.-M. Fedeli, Electrically driven hybrid Si/III-V Fabry-Pérot lasers based on adiabatic mode transformers. Opt. Express **19**, 10317 (2011).
4. D. Liang, M. Fiorentino, S. Srinivasan, J. E. Bowers, and R. G. Beausoleil, Low threshold electrically-pumped hybrid silicon microring lasers. IEEE J. Select. Topics Quantum Electronics **17**, 1528 (2011).
5. C. Zhang, D. Liang, G. Kurczveil, J. E. Bowers, and R. G. Beausoleil, Thermal management of hybrid silicon ring lasers for high temperature operation IEEE J. Sel. Top. Quantum Electron. **21**, 1502607 (2015).
6. V. Ya. Aleshkin, N. V. Baidus, A. A. Dubinov, A. G. Fefelov, Z. F. Krasilnik, K. E. Kudryavtsev, S. M. Nekorkin, A. V. Novikov, D. A. Pavlov, I. V. Samartsev, E. V. Skorokhodov, M. V. Shaleev, A. A. Sushkov, A. N. Yablonskiy, P. A. Yunin, and D. V. Yurasov, Monolithically integrated InGaAs/GaAs/AlGaAs quantum well laser grown by MOCVD on exact Ge/Si(001) substrate. Appl. Phys. Lett. **109**, 061111 (2016).
7. N. V. Kryzhanovskaya, E. I. Moiseev, Yu. S. Polubavkina, M. V. Maximov, M. M. Kulagina, S. I. Troshkov, Yu. M. Zadiranov, A. A. Lipovskii, N. V. Baidus, A. A. Dubinov, Z. F. Krasilnik, A. V. Novikov, D. A. Pavlov, A. V. Rykov, A. A. Sushkov, D. V. Yurasov, and A. E. Zhukov, Electrically pumped InGaAs/GaAs quantum well microdisk lasers directly grown on Si(100) with Ge/GaAs buffer. Opt. Express **25**, 16754 (2017).
8. T. Wang, H. Liu, A. Lee, and F. Pozzi, A. Seeds, 1.3-μm InAs/GaAs quantum-dot lasers monolithically grown on Si substrates. Opt. Express **19**, 11381 (2011).
9. A. D. Lee, Q. Jiang, M. Tang, Y. Zhang, A. J. Seeds, and H. Liu, InAs/GaAs quantum-dot lasers monolithically grown on Si, Ge, and Ge-on-Si substrates. IEEE J. Select. Topics Quantum Electron. **19**, 1901107 (2013).
10. S. Chen, W. Li, J. Wu, Q. Jiang, M. Tang, S. Shutts, S. N. Elliott, A. Sobiesierski, A. J. Seeds, I. Ross, P. M. Smowton, H. Liu, Electrically pumped continuous-wave III–V quantum dot lasers on silicon. Nat. Photon. **10**, 307 (2016).
11. R. Chen, T. T. D. Tran, K. W. Ng, W. S. Ko, L. C. Chuang, F. G. Sedwick, and C. J. Chang-Hasnain, Nanolasers grown on silicon. Nat. Photon. **5**, 170 (2011).
12. T. T. D. Tran, R. Chen, K. W. Ng, W. S. Ko, F. Lu, and C. J. Chang-Hasnain, Three-dimensional whispering gallery modes in InGaAs nanoneedle lasers on silicon. Appl. Phys. Lett. **105**, 111105 (2014).
13. Y. Wan, Q. Li, A. Y. Liu, and A. C. Gossard, J. E. Bowers, E. Hu, and K. M. Lau, Optically pumped 1.3 μm room-temperature InAs quantum-dot micro-disk lasers directly grown on (001) silicon. Opt. Lett. **41**, 1664 (2016).
14. Y. Wan, J. Norman, Q. Li, M. J. Kennedy, D. Liang, C. Zhang, D. Huang, A. Y. Liu, A. Torres, D. Jung, A. C. Gossard, E. L. Hu, K. M. Lau, and J. E. Bowers, Sub-mA threshold 1.3 μm CW lasing from electrically pumped micro-rings grown on (001) Si. CLEO: Applications and Technology 2017, San Jose, CA, USA, May 14–19, 2017, paper JTh5C.3.
15. N. V. Kryzhanovskaya, E. I. Moiseev, Yu. V. Kudashova, F. I. Zubov, A. A. Lipovskii, M. M. Kulagina, S. I. Troshkov, Yu. M. Zadiranov, D. A. Livshits, M. V. Maximov, and A. E. Zhukov, Continuous-wave lasing at 100°C in 1.3 μm quantum dot microdisk diode laser. Electron. Lett. **51**, 1354 (2015).
16. M. V. Maximov, N. V. Kryzhanovskay, A. M. Nadtochiy, E. I. Moiseev, I. I. Shostak, A. A. Bogdanov, Z. F. Sadrieva, A. E. Zhukov, A. A. Lipovskii, D. V. Karpov, J. Laukkanen, and J. Tommila, Ultrasmall microdisk and microring lasers based on InAs/InGaAs/GaAs quantum dots. Nanoscale Res. Lett. **9**, 657 (2014).
17. N. V. Kryzhanovskaya, A. E. Zhukov, M. V. Maximov, E. I. Moiseev, I. I. Shostak, A. M. Nadtochiy, Yu. V. Kudashova, A. A. Lipovskii, M. M. Kulagina, and S. I. Troshkov, . Room temperature lasing in 1 μm microdisk quantum dot lasers. IEEE J. Select. Topics Quantum Electron. **21**, 1900905 (2015).
18. M. Tang, S. Chen, J. Wu, Q. Jiang, K. Kennedy, P. Jurczak, M. Liao, R. Beanland, A. J. Seeds, and H. Liu, Optimizations of defect filter layers for 1.3-μm InAs/GaAs quantum-dot lasers monolithically grown on Si substrates. IEEE J. Select. Topics Quantum Electronics **22**, 1900207 (2016).
19. D. Ouyang, N. N. Ledentsov, D. Bimberg, A. R. Kovsh, A. E. Zhukov, S. S. Mikhrin, and V. M. Ustinov, High performance narrow stripe quantum-dot lasers with etched waveguide. Semicond. Sci. Technol. **18**, L53 (2003).
20. N. V. Kryzhanovskaya, E. I. Moiseev, Yu. S. Polubavkina, F. I. Zubov, M. V. Maximov, A. A. Lipovskii, M. M. Kulagina, S. I. Troshkov, V.-M. Korpijarvi, T. Niemi, R. Isoaho, M. Guina, M. V. Lebedev, T. V. Lvova, and A. E. Zhukov, Microdisk lasers based on GaInNAs(Sb)/GaAs(N) quantum wells. J. Appl. Phys. **120**, 233103 (2016).
21. N. V. Kryzhanovskaya, M. V. Maximov, S. A. Blokhin, M. A. Bobrov, M. M. Kulagina, S. I. Troshkov, Yu. M. Zadiranov, A. A. Lipovskii, E. I. Moiseev, Yu. V. Kudashova, D. A. Livshits, V. M. Ustinov, and A. E. Zhukov, Microdisk injection lasers for the 1.27-μm spectral range. Semiconductors **50**, 390 (2016).
22. M.-H. Mao, H.-C. Chien, J.-Z. Hong, and C.-Y. Cheng, Room-temperature low-threshold current-injection InGaAs quantum-dot microdisk lasers with single-mode emission. Opt. Express **19**, 14145 (2011).
23. M. Munsch, J. Claudon, N. S. Malik, K. Gilbert, P. Grosse, J.-M. Gerard, F. Albert, F. Langer, T. Schlereth, M. M. Pieczarka, S. Hofling, M. Kamp, A. Forchel, and S. Reitzenstein, Room temperature, continuous wave lasing in microcylinder and microring quantum dot laser diodes. Appl. Phys. Lett. **100**, 031111 (2012).
24. A. E. Zhukov, N. V. Kryzhanovskaya, M. V. Maximov, A. A. Lipovskii, A. V. Savelyev, I. I. Shostak, E. I. Moiseev, Yu. V. Kudashova, M. M. Kulagina, and S. I. Troshkov, Thermal resistance of ultra-small-diameter disk microlasers. Semiconductors **49**, 674 (2015).